TOF Electron Energy Analyzer for Spin and Angular Resolved Photoemission Spectroscopy.

G. Lebedev, C. Jozwiak, N. Andresen, A. Lanzara, Z. Hussain

Lawrence Berkeley National Laboratory,
One Cyclotron Rd. MS: 7-222, Berkeley, CA, 94720, USA
Email: gvlebedev@lbl.gov, Phone: (510) 486-4262

Abstract

Current pulsed laser and synchrotron x-ray sources provide new opportunities for Time-Of- Flight (TOF) based photoemission spectroscopy to increase photoelectron energy resolution and efficiency compared to current standard techniques. The principals of photoelectron timing front formation, temporal aberration minimization, and optimization of electron beam transmission are presented. We have developed these concepts into a high resolution Electron Optical Scheme (EOS) of a TOF Electron Energy Analyzer (TOF-EEA) for photoemission spectroscopy. The EOS of the analyzer includes an electrostatic objective lens, three columns of transport lenses and a 90 degree energy band pass filter (BPF). The analyzer has two modes of operation: Spectrometer Mode (SM) with straight passage of electrons through the EOS undeflected by the BPF, allowing the entire spectrum to be measured, and Monochromator Mode (MM) in which the BPF defines a certain energy window inside the scope of the electron energy spectrum.

I. Introduction

Photoemission spectroscopy is a general term for techniques based on the photoelectric effect explain by Einstein [1], in which light with photon frequency ν hits a sample and causes the emission of an electron with kinetic energy $E_k = h\nu - \Phi$, where Φ is the sample's work function. The measurement of the energy spectrum of emitted electrons as a function of emission angle is the goal of Angle-Resolved Photoemission Spectroscopy (ARPES), which provides a mapping of the electronic structure of a solid. The current major requirements for new ARPES instrumentation [2] are:

1. energy resolution better than one meV within a kinetic energy range of 20-200 eV,
2. variable acceptance angle of 1-10 degrees with angle resolution better than 0.1 degrees.

Two major concepts are currently used for designing static Electron Energy Analyzers (EEA), either hemispherical or cylindrical EEA. In contrast to these techniques, the TOF concept determines the energy of electrons by determining their precise arrival time at an electron detector from a pulsed source of electrons. The advantage of a TOF-EEA is a significantly wider window of simultaneously detected energies and EOS stigmatic properties that avoid analyzer transmission calibration in two perpendicular directions. Due to the short pulse nature of photoelectron excitation

required by TOF spectrometers, they are natural choices for researching time dependant processes. TOF analytical methods are widely used in high resolution mass-spectroscopy, originally introduced by Wiley and McLaren [3]. In this case, a significant increase in resolving power is achieved by compensation of chromatic aberration, or energy spread of the ion beam, in the analyzer through the use of electrostatic mirrors. However, in photoemission spectroscopy the energy spread of the electron beam is the measured parameter and chromatic aberration of the electron optical system is the dispersion parameter of the instrument. One of the first designs of a TOF-EEA for surface-science applications was introduced by Bachrach et al. [4], and was later enhanced for gas-phase samples [5].

II. Main design concepts of TOF electron energy analyzer

One of the major criteria for designing a TOF-EEA is the condition that two consecutive bunches of electrons emitted from the specimen cannot overlap at the detector plane. This places restrictions on either the period of the pulsed excitation source or the range of initial electron energies passing though the analyzer. For example, the Advanced Light Source (ALS) synchrotron in Berkeley, CA can operate in a so-called "two-bunch" mode which generates UV and X-ray pulses of 70 pS width and a window of time between pulses (bunch time) of t_b = 328 ns. In a photoemission experiment, the emitted electron's total energy spectrum range is governed by the wavelength of incident light, ν, and encompasses energies

$$\varepsilon_{0\min} = 0 \text{ to } \varepsilon_{0\max} = h\nu - \varepsilon_w \quad (1)$$

where ε_w is the work function of the sample. After acceleration of the beam by adding energy ε_u, the energy spread will be:

$$\Delta\varepsilon \subset [\varepsilon_{1\min} = \varepsilon_u, \varepsilon_{1\max} = \varepsilon_u + \varepsilon_{0\max}].$$

In this case, the condition of separation of electron packages can be expressed as:

$$t_1(\varepsilon_{1\min}) \le t_2(\varepsilon_{1\max}) + t_b \quad (2)$$

From energy conservation, the time propagation of a charged particle through an analyzer on the optical axis Z can be expressed as:

$$t_a = \frac{1}{\sqrt{2\eta}} \int_0^z \frac{1}{\sqrt{\Phi(z) + \varepsilon_0}} dz \quad (3)$$

where $\Phi(z) = U(0,0,z)$ is the electrical potential along the optical axis Z of the EOS, ε_0 is initial energy of the charged particle beam, and $\eta = e/m$, the charge to mass ratio

of the charged particle. If we introduce equivalent drift space energy ε_d to be defined as the energy of a charged particle that travels through a drift space of length L in the same amount of time it would take to propagate through an EOS of equal length, we have:

$$\varepsilon^d = (L / \int_0^L \frac{1}{\sqrt{\Phi(z) + \varepsilon_0}} dz)^2$$

Condition (2) can now be expressed as:

$$\frac{\varepsilon^d_{\max}}{\varepsilon^d_{\min}} \le (1 - \sqrt{x})^{-2} \equiv F(x) \qquad (4)$$

where $x = \varepsilon^d_{\min} / \varepsilon^d_b$ is the ratio of the minimum drift equivalent energy and bunch time equivalent energy ($\varepsilon^d_b = L^2 / 2\eta t_b^2$). The function F(x) is presented in Fig.1.

As an example, for a drift space L=1m and bunch time $t_b = 328nS$ (ALS "two-bunch" mode), the bunch time equivalent drift space energy is $\varepsilon^d_b = 32eV$. For a minimum drift space energy of $\varepsilon^d_{\min} = 10eV$, Eq. (4) gives $\varepsilon^d_{\max} = 51.4eV$. This bandwidth can be satisfied if the photon energy used is below 50 eV. Otherwise the analyzer must have an energy band pass filter to narrow the electron energy bandwidth such that condition (2) is satisfied. Fig. 2 graphs the maximum $\varepsilon^d_{\max}$ as a function of $\varepsilon^d_{\min}$ for the assumed ε^d_b of 32 eV according to Eq. (4).

The specific EOS of our developed TOF-EEA consists of a set of axially symmetric electrostatic lenses (Fig. 3), a stigmatic 90 degree energy BPF, a number of corrective elements (quadruple deflectors), a variable aperture placed after the objective lens, and a variable slit mounted on the front of the focusing lens of the second lens column downstream of the BPF. The analyzer has two modes of operation:

1. Spectrometer Mode (SM) - the BPF is inactive and the electron beam passes through Lens Column (LC) 1 and 3. In this case the entire photoemission spectrum is recorded at once.
2. Monochromator Mode (MM)- the BPF is active and electron beam passes through LC1 and LC2. The energy bandwidth of the successfully transported electron beam is defined by the BPF pass energy and the width of the variable slit.

At the end of LC2 is an exchange-scattering electron spin detector [6], and a compact fast MCP electron detector assembly (Hamamatsu F4655-12) is attached to the end of LC3.

The major criteria for optimizing the EOS of the analyzer were maximizing the energy resolution and transmission of the electron beam. According to these requirements, three immersion objective lenses were designed to allow acceleration or deceleration of the electron beam to a specified energy. Photoelectrons from the sample have a relatively wide energy spread, and so the EOS cannot achieve maximum transmission for the entire

range simultaneously. For MM operation the energy window from the photoemission spectrum is controlled by the BPF and variable slit located in the focal plane of Transport Lens 3 of LC2.

III. Energy resolution of TOF-EEA:

The first order variation of electron time propagation along the optical axis of the EOS is expressed as

$$\Delta t_a = < t \mid 001 > \Delta \varepsilon_0 \qquad (5)$$

where $< t \mid 001 >$ is the coefficient of the first order temporal aberration of the EOS and $\Delta \varepsilon_0$ is the initial energy spread. Integral Eq. (3) defines the relationship between the initial energy of an electron and its flight time through the analyzer along the optical axis as a function $t_a = F(\varepsilon_0)$. Accordingly, the initial energy of the electron can be expressed as an inverse function of its flight time:

$$\varepsilon_0 = F^{-1}(t_a) \qquad (6)$$

From (5) and (6) the energy resolution of the analyzer can be presented as:

$$RES = \frac{\Delta \varepsilon}{\varepsilon_0} = \frac{\Delta t}{< t \mid 001 > F^{-1}(t_a)} \qquad (7)$$

For a drift space, Eq. (7) transforms to: $RES_{drift} = \frac{\Delta \varepsilon_0}{\varepsilon_0} = \frac{2\Delta t_a}{t_{drift}}$

In a real device, the time variation on the detector, Δt, depends not only on the EOS temporal aberrations Δt_{EOS}, but also other factors such as detector jitter Δt_d, the pulse width of electron source Δt_s, DAQ timing resolutions Δt_q, the presence of residual magnetic fields Δt_m, parasitic EOS element displacement aberrations, and others. This means the overall arrival time deviation on the TOF detector can be expressed as:

$$\Delta t = \sqrt{\Delta t_{EOS}^2 + \Delta t_q^2 + \Delta t_d^2 + \Delta t_s^2 + \Delta t_m^2 + \ldots}$$

The EOS should be designed such that Δt_{EOS} is minimized for all modes of analyzer operation and parameters.

IV. Temporal Aberrations of TOF_EEA

From energy conservation, the time propagation of a nonrelativistic charged particle with initial energy ε_0 and energy spread $\Delta\varepsilon_0$ in the plane of the curvilinear optical axis OZ can be expressed as:

$$t = \frac{1}{\sqrt{2\eta}} \int_0^L \frac{\sqrt{[1-k(z)x(z)]^2 + x'^2(z) + y'^2(z)}}{\sqrt{U(x,y,z) + \varepsilon_0 + \Delta\varepsilon_0}} dz \qquad (8)$$

where $U(x,y,z)$ denotes the potential distribution along axis OZ with curvature k(z), and x(z) and y(z) are the trajectories of the electrons in the azimuthal and axial planes accordingly. The initial coordinates of the charged particle upon entrance to the EOS can be expressed as a vector:

$$S_0 = \begin{pmatrix} x_0' \\ x_0 \\ y_0' \\ y_0 \\ \Delta\varepsilon_0 \end{pmatrix}.$$

Eq. (8), to second order in initial trajectory parameters, can be presented as:

$$t = < t \mid 000 > + T^{(1)} S_0 + S_0^t T^{(2)} S_0 \qquad (9)$$

where $< t \mid 000 >$ is the time propagation of a particle along of optical axis OZ and $T^{(1)}$ and $T^{(2)}$ are the temporal aberration matrices of first and second order respectively.

For an axially symmetric EOS,

$$T^{(1)} S_0 = < t \mid 001 > \Delta\varepsilon_0$$

$$S_0^t T^{(2)} S_0 = < t \mid 002 > \Delta\varepsilon_0^2 + P_0^t Q P_0$$

and so (9) then takes the form:

$$t = <t \mid 000> + <t \mid 001> \Delta\varepsilon_0 + <t \mid 002> \Delta\varepsilon_0^2 + P_0^t Q P_0 \qquad (10)$$

where $< t \mid 001 >$ and $< t \mid 002 >$ are the first and second order temporal aberrations due to energy spread, the vector $P_0 = \begin{pmatrix} r_0' \\ r_0 \end{pmatrix}$ is the initial phase coordinate vector and $Q = \begin{pmatrix} < t \mid 200 > & < t \mid 110 > \\ < t \mid 110 > & < t \mid 020 > \end{pmatrix}$ is the matrix of second order geometric temporal aberrations. For electrostatic axially symmetric systems, the second order geometric temporal aberrations are derived from the following aberration generating-function:

$$< t \mid , , 0 >= \frac{1}{\sqrt{2\eta}} \int_0^z [\frac{1}{2\Phi(z)^{1/2}} r'^2 - \frac{\Phi'(z)}{4\Phi(z)^{3/2}} r' r + \frac{3\Phi'(z)^2}{16\Phi(z)^{5/2}} r^2] dz$$

The expression under the integral is a positively defined quadratic form of the paraxial trajectory r(z) and its derivative r'(z). This means the temporal aberrations in Q are positive for any initial parameters of a charged particle and can be zero only for a beam with null coordinate and angle spread. At the same time, on the phase space P_0, the second order temporal aberrations $P_0^t Q P_0$ in Eq. (10) present a family of ellipses with two geometric factors: the angle of axis rotation,

$$\Theta = \frac{1}{2} \tan^{-1}[< t \mid 110 > / (< t \mid 200 > - < t \mid 020 >)] \qquad (11)$$

and the ratio of semimajor q_1 and semiminor axis q_2,

$$D = q_1 / q_2 = \sqrt{\lambda_2 / \lambda_1} \qquad (12)$$

equal to the square root of the ratio of eigenvalues λ_1, λ_2 of the matrix Q in Eq. (10). Parameters (11) and (12) define a shape of acceptance of the EOS on the phase space P_0 in which the minimum timing distortion is realized for maximum transmission of the electron beam.

In most practical cases, the emittance of the beam from the sample plane has a small coordinate spread relative to the inner diameter of the EOS ($r_0 << 1$). Then the timing fronts of electrons near the optical axis at some detector plane $z = z_d$ will have parabolic form, which can be expressed in the form:

$$Z(r) = \sqrt{2\eta\varepsilon_d} \frac{< t \mid 200 >_{z=z_d}}{r_\alpha^2(z_d)} r^2 \qquad (13)$$

where ε_d is the energy and r_α is the paraxial trajectory coordinate with initial parameters $r_\alpha(0) = 0, r_\alpha'(0) = 1$. Fig. 5 shows the calculated timing fronts for an

example of an axially symmetric three electrode lens. Actually, expression (13) defines the shape of a detector surface with which the impact of temporal aberration of the EOS is a minimum.

V. Constructing energy spectrum of TOF-EEA

The relation between the arrival time on the detector, t, and the energy of the electron at the sample plane, ε_0, is expressed by the transcendental Eq. (3) . This equation can be solved at each t by standard numerical methods, but requires significant calculation time. It is more efficient to use the second order polynomial approximation from Eq. (10)

$$t^{(2)} = <t|000> + <t|001>\Delta\varepsilon_0 + <t|002>\Delta\varepsilon_0^2 \qquad (14)$$

Then the initial energy of the electron within a specified energy window can be found directly as a solution to the quadratic Eq. (14). If the polynomial coefficients in (14) are pre-calculated from the EOS model and stored in the EOS lens tables, one has an effective run-time algorithm for time-to-energy conversion.

The relative error between the exact and approximate values

$$ERR(\varepsilon_0) = [\varepsilon(t_a) - \varepsilon(t^{(2)})] / \varepsilon(t_a) \qquad (15)$$

is calculated for an axially symmetric Einzel lens with radius R=1, length of middle electrode L=2, and potential of middle electrode V and presented in Fig. 6. We can see that it strongly depends on lens excitation and is significantly smaller in acceleration lens mode (V > 1).

VI. Electronic and computer control

The analyzer has two TOF detectors, one for SM operation based on the commercially available Hamamatsu F4655-12 MCP assembly, and the second for MM operation which is an LBNL design with a center-hole in both the anode and MCP. In this second detector, electrons pass through the 6 mm hole in the detector and backscatter from a target [6] before striking the detector. Both detectors feed their signal into the ORTEC 9327 Amplifier/Timing Discriminator and ORTEC 9308 Picosecond Time Analyzer for signal processing (Fig. 7). High voltages power supplies for powering the lenses and detectors were built by Gammadata Scienta Inc. and are controlled by computer through USB interface. Software for controlling the analyzer was developed at LBNL and includes several major modules:

1. "EOS SIMULATOR" – simulates flow of charge particle through a sequence of electrostatic elements. Calculates major temporal aberrations and statistical parameters of the electron beam.
2. "LENS TABLE EDITOR"- creates and stores calibrated lens voltages for given pass energies of the analyzer.

3. "EXPERIMENT PROCESSOR" – runs experiment with specified parameters.
4. "SPECTRUM MANAGER" – stores accumulated photoelectron spectrum in user specified format. The software allows users to collect electron energy spectrum in two modes:
    1. Snapshot – the entire energy spectrum is collected in specified energy window.
    2. Scan – the energy window moves through the spectrum with specified step size.

VII. Experimental setup and results

Lens column 1 (Fig. 3) of the TOF-EEA was used as prototype for testing its analytical parameters and controlling software on beamline 12.0.1 at the LBNL Advance Light Source during "two-bunch" mode operation. The sample used was a polycrystalline gold film evaporated *in-situ* on a copper substrate directly attached to a liquid He cryostat. The sample was cooled down to 20K. Fig. 8 shows the photoelectron spectrum collected using 60 eV photons and the entire analyzer grounded to be pure drift space. Fig. 9 shows a small window of the photoelectron spectrum centered on the Fermi edge collected using 30 eV photons and the analyzer set to a pass-energy ~10 eV. The photon spot size on the sample was approximately 2 mm and photon pulse duration was estimated as 100 pS.

The energy resolution of the analyzer was calculated based on measuring the Fermi-Dirac distribution of the Fermi edge of the sample and can be estimated as

$$\Delta E_{FD}^{m\ 2} = \Delta E_{FD}^2 + \Delta E_{h\nu}^2 + \Delta E_t^2 + \Delta E_{EEA}^2$$

where $\Delta E_{FD} = 4kT$ is the FWHM temperature broadened Fermi-Dirac distribution, $\Delta E_{h\nu}$ is photon beam energy resolution, ΔE_t is energy broadening of TOF-EEA due the finite duration of pulsed photon source, and ΔE_{EEA} is the contribution of analyzer itself. Figure 10 shows that an energy resolution of approximately 30 meV was achieved at a pass-energy ~10 eV, which is good agreement with simulated data in Fig. 10 for specified parameters of experiment.

VIII. Conclusion

We have shown the concepts behind a Time-of-Flight based photoelectron energy analyzer. The theory of the TOF technique is described, and an efficient and accurate approach to the important time-to-energy conversion is presented. Preliminary tests of a prototype TOF-EEA has shown that theoretical estimation of analytical parameters is in good agreement with experimental data. For an illuminated spot size of 0.3 mm and a photon pulse duration of 70 pS we expect the complete system TOF-EEA to achieve submilivolt energy resolution in both Spectrometer and Monochromator Modes of operation.

This work was supported by US DOE Contract No DE-AC02-05CH11231.

X. References

[1] Einstein, A., Ann. Physik **31**, 132 (1905)
[2] Damascelli A., Physica Scripta., Vol. T109, 61-74, 2004
[3] W.C.Wiley, I.H.McLaren, Rev.Sci. Instrum., **26** (1955), 1150
[4] R.Z.Bachrach, F.C.Brown, and S.B.M.Hagstrom, J.Vac.Sci.Technol. **12**, 309 (1975)
[5] O.Hemmers, S.B.Whitfield, P.Glans, H.Wang, and D.W.Lindle, Rev. Sci.Instr. **69**, (1998), 3809
[6] J. Graf, C. Jozwiak, A. K. Schmid, Z. Hussain, and A. Lanzara, Physical. Rev. B **71**, 144429 (2005)

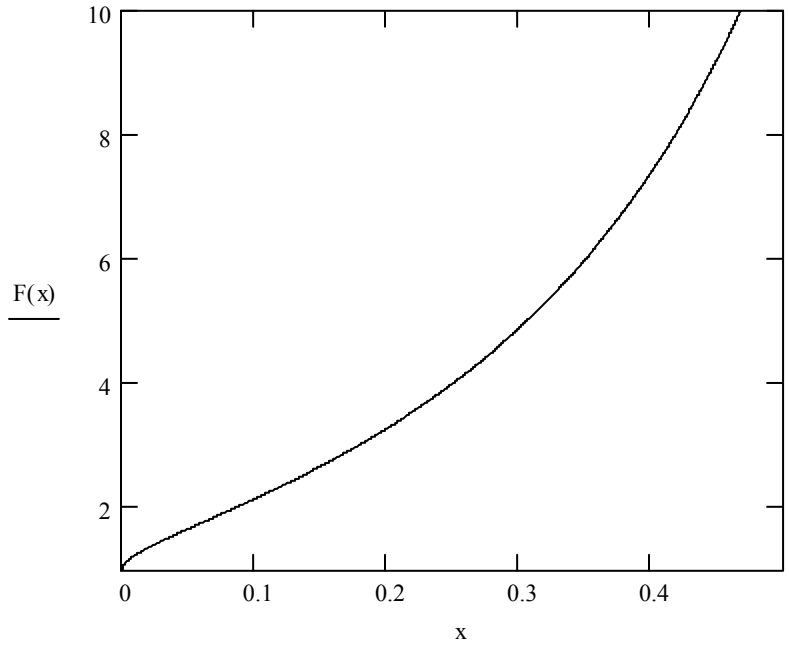

FIG. 1. Non-overlapping energy scale as function of normalized minimum initial energy of photoelectrons.

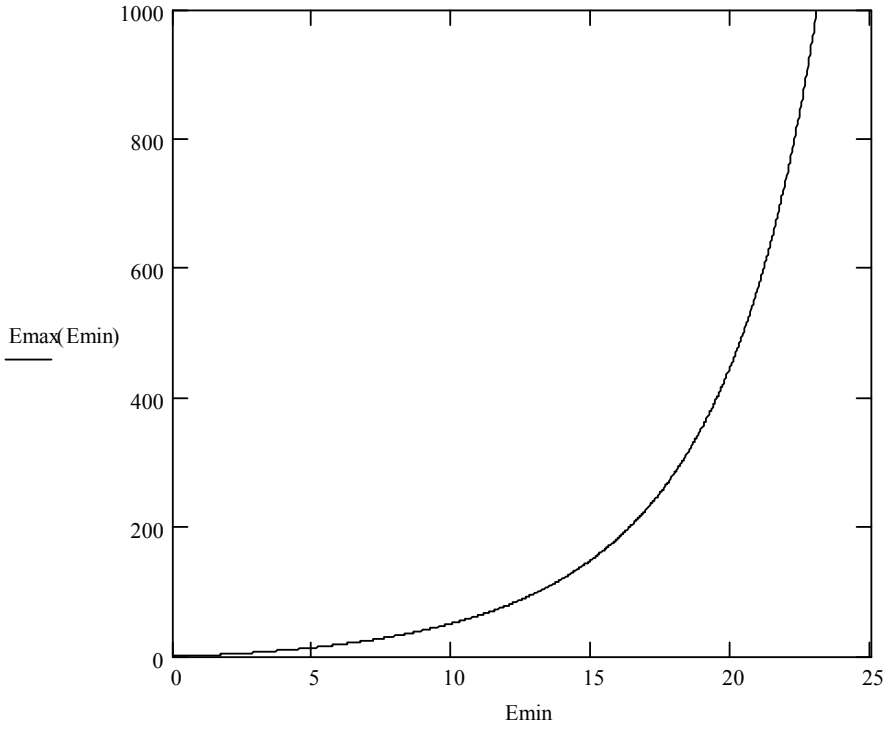

FIG. 2. Maximum (non-overlapping bunch condition) of drift energy as function of minimum initial energy of photoelectrons for $\varepsilon_b^d = 32eV$.

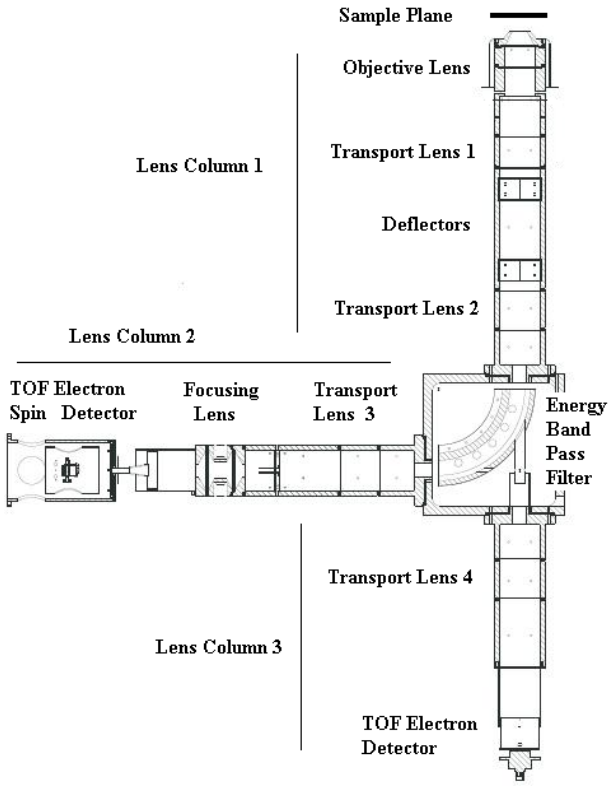

FIG. 3 Electron Optical Scheme of TOF Electron energy analyzer

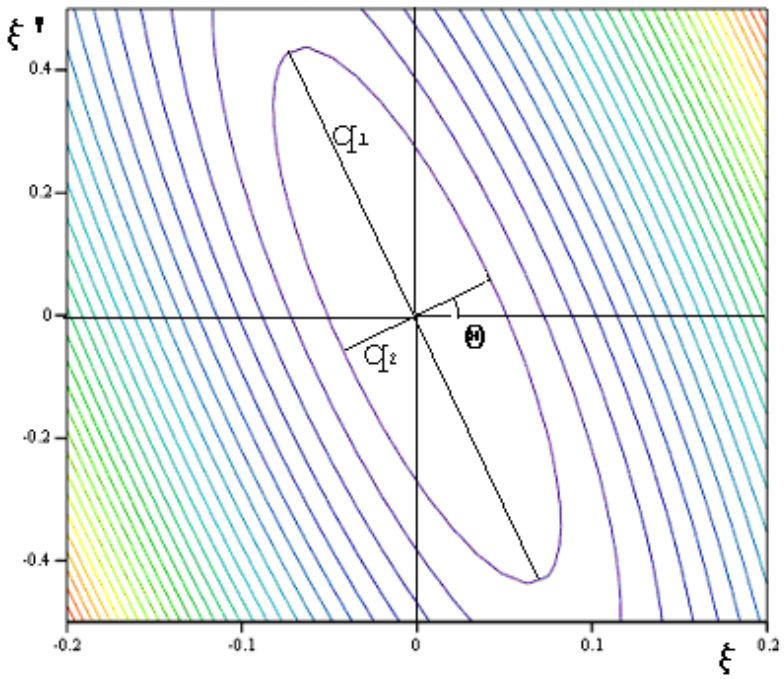

FIG.4. Equal line map of temporal aberration on phase coordinate plane P_0.

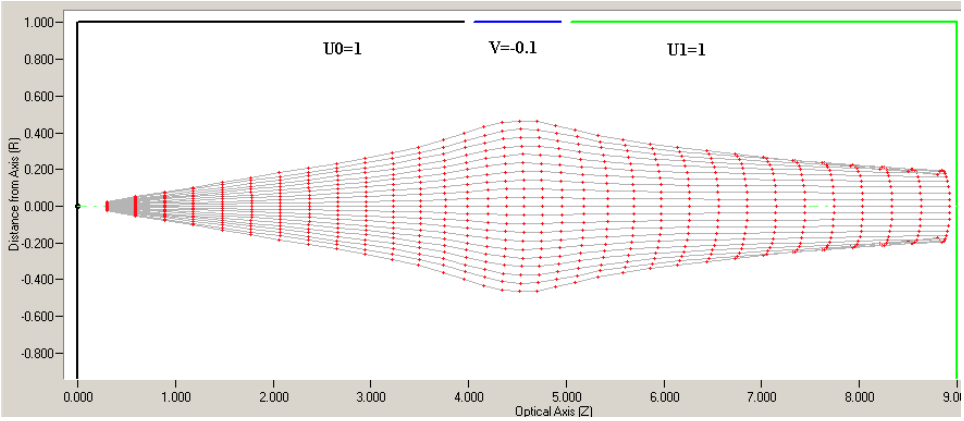

FIG.5. Timing front formation in three electrode axially symmetric lens.

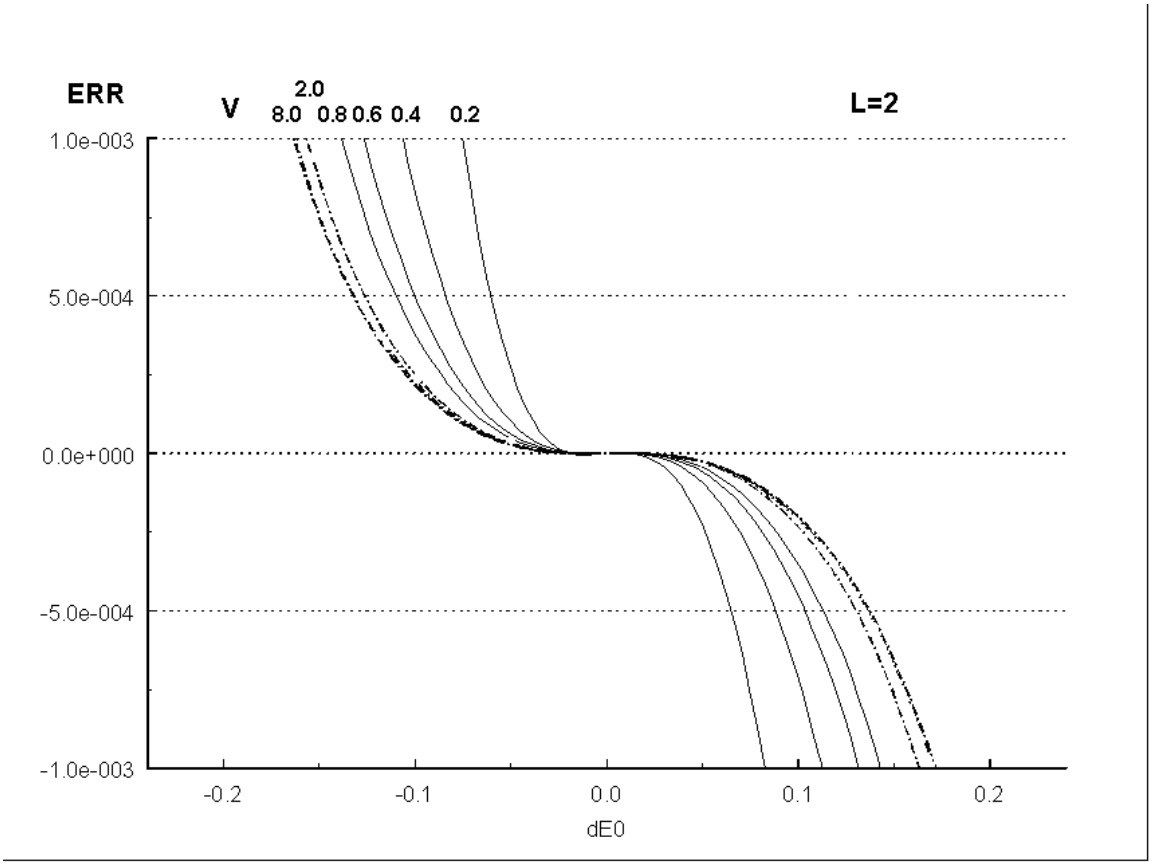

FIG. 6. Error of exact and approximated time-to-energy conversion (15) for Einzel tube lens radius R=1 , length L=2 and potential of middle electrode V

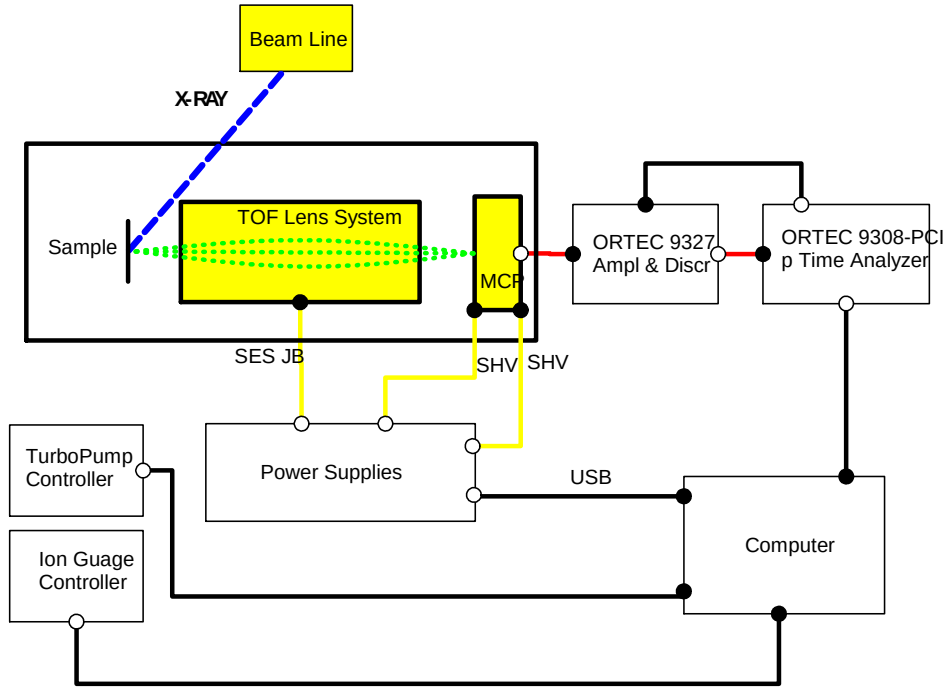

FIG. 7. Conceptual scheme of data acquisition and electronic control of TOF-EEA.

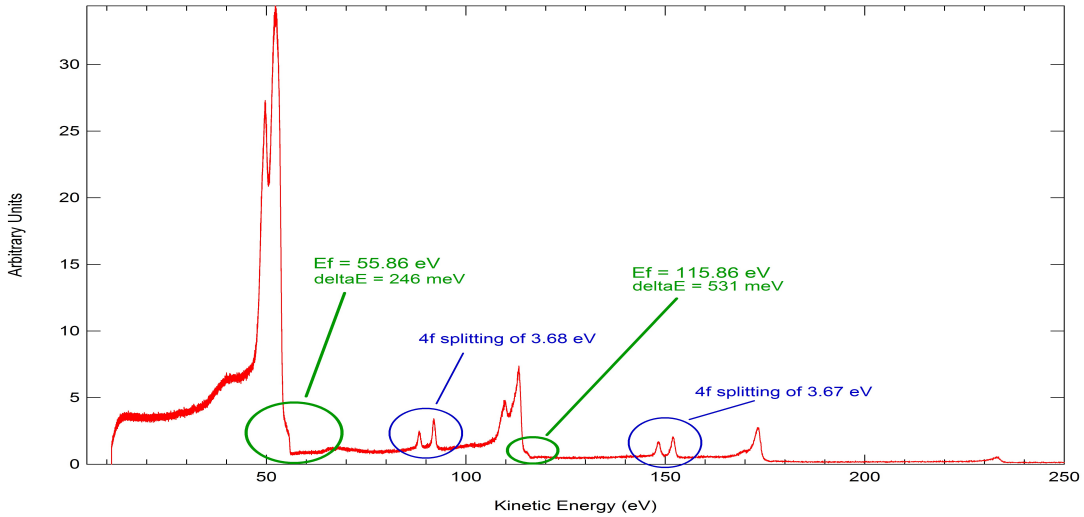

FIG. 8 TOF Au spectrum translated to energy scale. Photon energy = 60 eV, and lens system was grounded for pure drift space. Higher order light (120 eV, 180eV, etc) produce the repeating sets of peaks at successively higher kinetic energies.

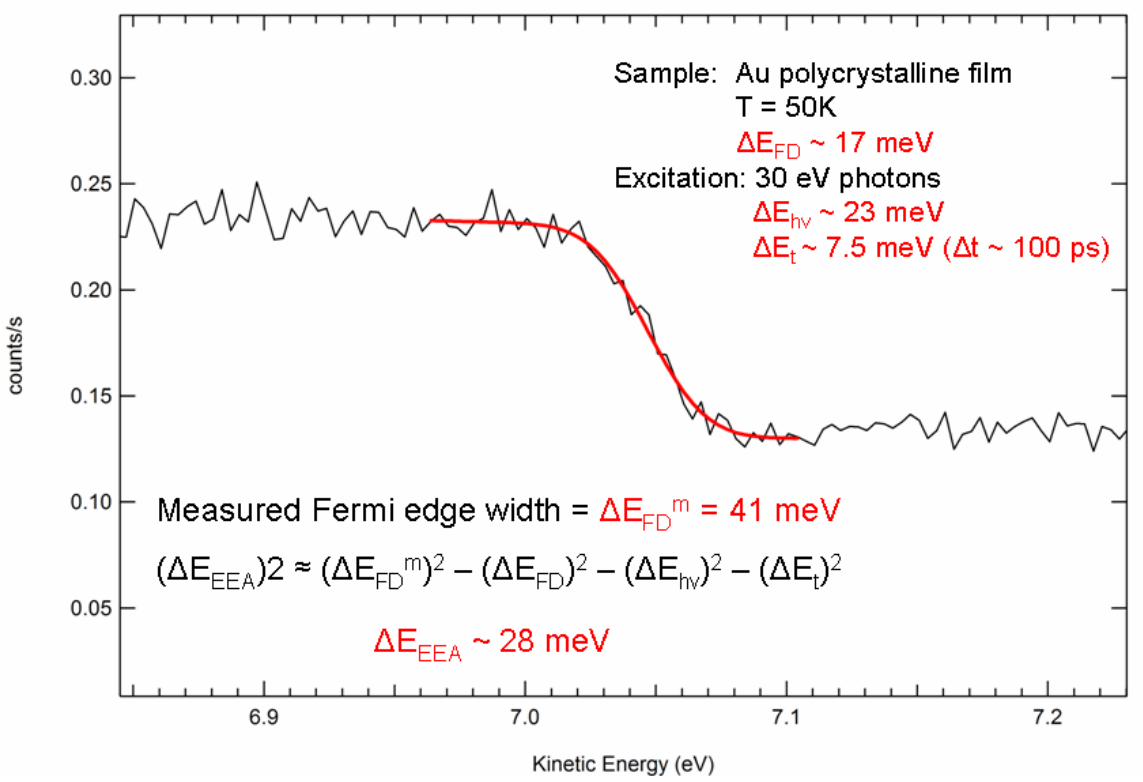

FIG. 9 TOF Au spectrum Fermi edge translated to energy scale. Photon energy = 30 eV and pass energy was ~10eV. Fitting the measured Fermi edge and following the text, the energy resolution of the EEA was found to be approximately 28 meV.

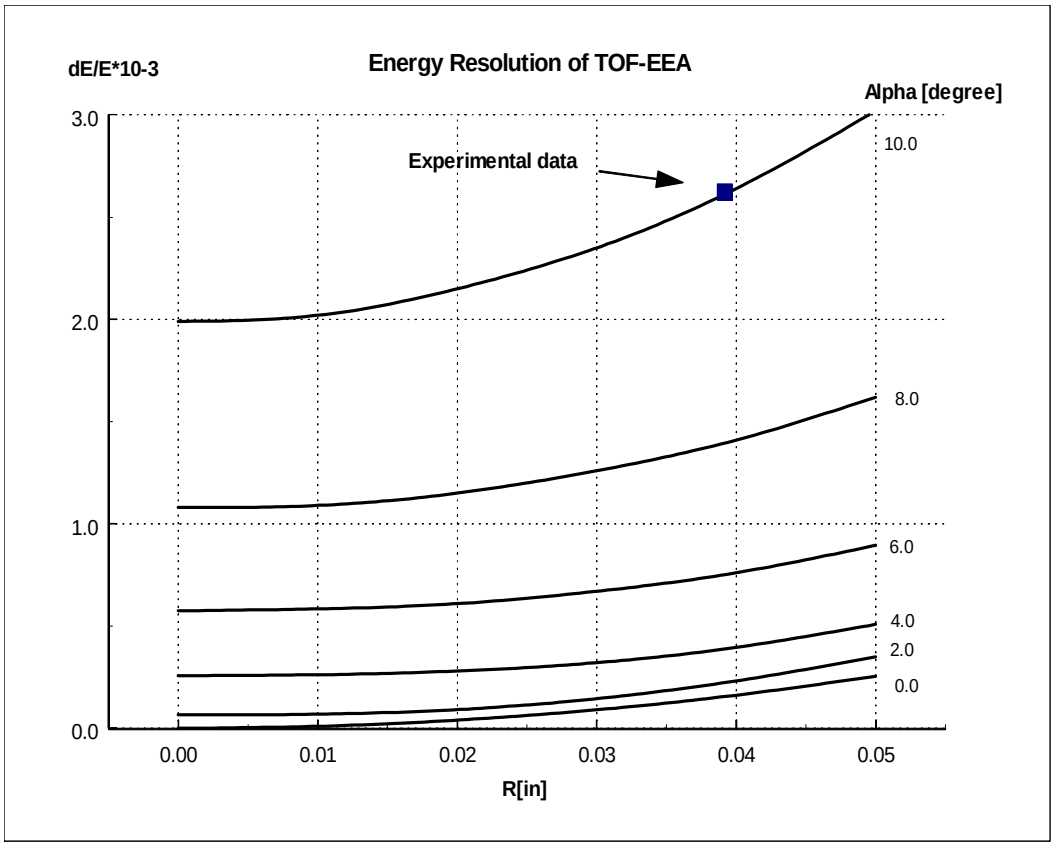

FIG.10 Energy resolution of TOF-EEA "Prototype" as a function of x-ray spot radius (R) on the sample at different acceptance angles (Alpha) of analyzer from simulation. Experimental data point from FIG. 9.